Novel insights into old anticancer drugs
Zanden, S.Y. van der

Cover Page

Universiteit Leiden

Author: Zanden, S.Y. van der
Title: Novel insights into old anticancer drugs
Issue date: 2021-03-02
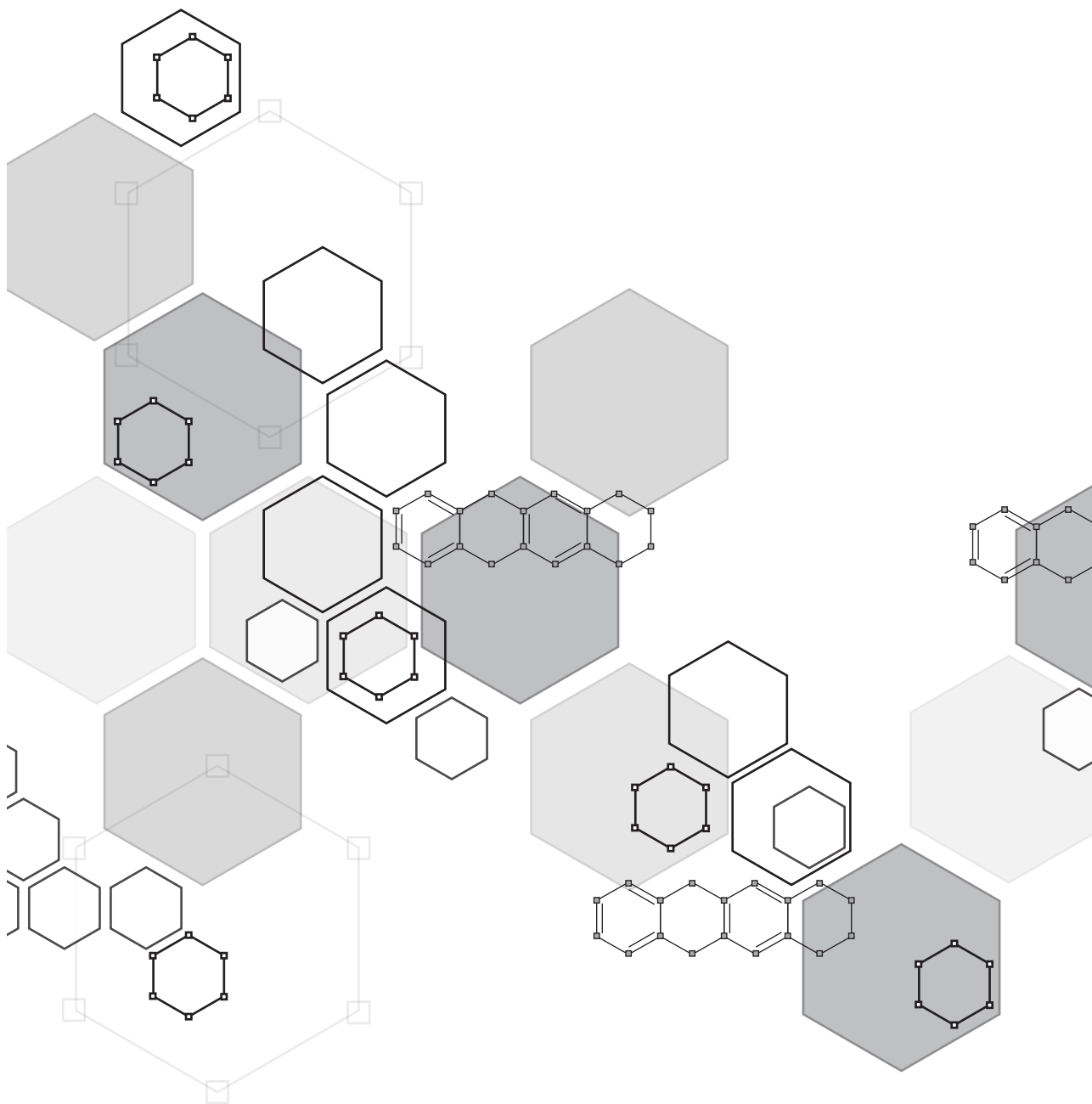
Exploring the chemical space around the 3' amine of doxorubicin for improved cytotoxic drugs with different genomic specificity

6

Sabina Y. van der Zanden, Feija L. Hamoen, Daniel Borràs, Dennis P. A. Wander, Herman S. Overkleeft, Jeroen D. C. Codée, Baoxu Pang, Jacques Neefjes

ABSTRACT

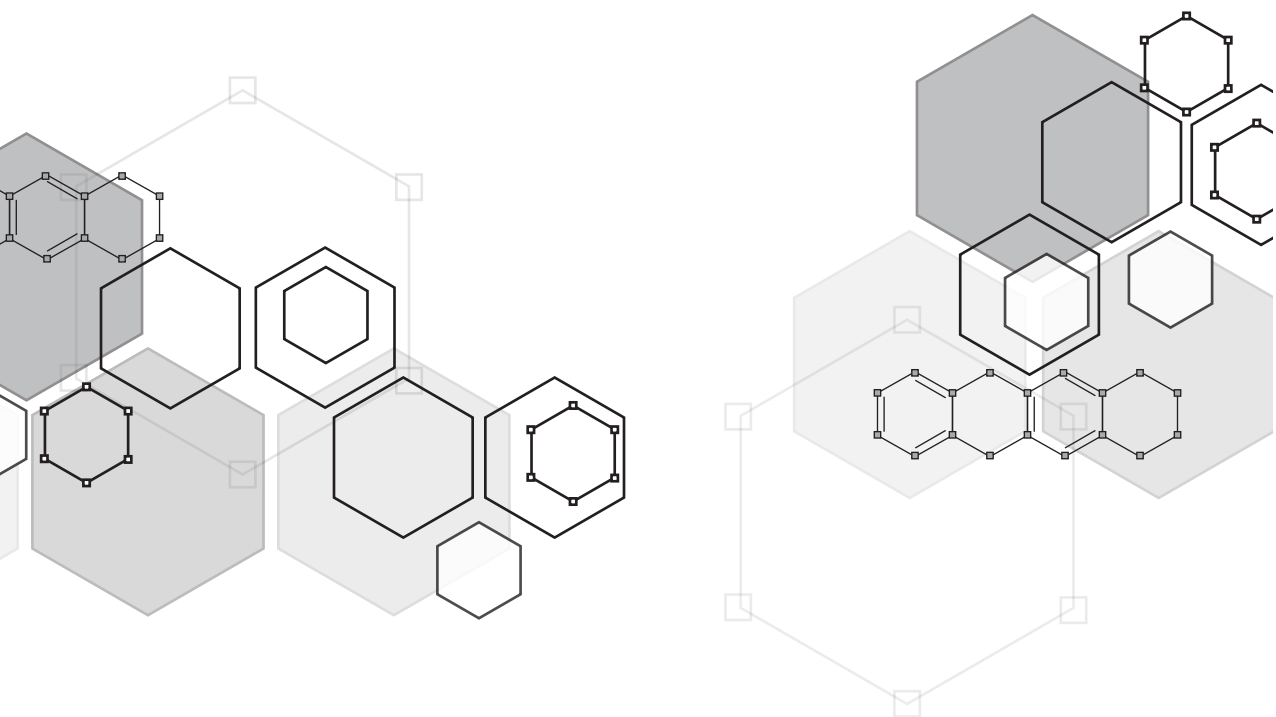The anthracycline drug doxorubicin is a very effective anticancer drug for different types of solid and hematological tumors. However, treatment coincides with severe adverse effects. Although hundreds of anthracycline analogs are either isolated from natural or mutant sources, or prepared via organic synthesis with the aim to find novel anticancer therapies without toxicities, limited drugs made it into clinic. Therefore, a better understanding of the molecular mechanism of actions, and a clear structure-function relationship for these drugs would benefit the search for new therapies. Recently, chromatin damage via eviction of histones was discovered as a novel mechanism of action, and we have shown that the amino sugar is important for this activity. Based on this new knowledge, we synthesized and evaluated a set of doxorubicin analogs varying at the 3' position, to further investigate the structure-function relationship of the anthracyclines. We show that the bulky tertiary amine at the 3' position is responsible for the effective histone evicting activity, which correlates with low IC_{50} values in various tumor cell lines. On the contrary, the absence of the amine at this position result in effective DNA damaging compounds without chromatin damage activity. Furthermore, by chemically modifying the amino sugar of doxorubicin, the genomic locations of these drugs, in terms of chromatin damage and/or targeting topoisomerase IIα, are also altered. The chemical space around the 3'position of doxorubicin's sugar moiety includes variants with higher cytotoxicity and a different genomic selectivity than their parental drug.

INTRODUCTION

Anthracycline drugs, including doxorubicin, belong to the most used and effective anticancer drugs. However, treatment containing these drugs is plagued by severe adverse effect [1, 2]. To overcome these side effects, thousands of anthracycline analogs have been made with the aim to develop effective treatment with limited toxicity, but only few drugs have entered the clinic [3]. For decades, formation of DNA double-strand breaks via interreference with the catalytic cycle of topoisomerase IIα (Topo IIα) was considered the major mechanism of action of these drugs [4]. Recently, a second mechanism of action was discovered, namely, chromatin damage via eviction of histones [5-7]. We showed that chromatin damage is a major mechanism by which these drugs initiate tumor cell killing, since analogs only able to evict histones are also effective anticancer drugs *in vitro* and *in vivo* [8]. In addition, separation of these two activities resulted in drugs with reduced toxicity. This novel insight can help in the development of new anthracycline analogs for improved cancer therapy. Further data suggest, that the modification, position and orientation of the amine on the sugar moiety of these anthracycline drugs are responsible for its combined biological activity [9, 10]. Methylation and the equatorial position of the amine enhances both cellular uptake and histone eviction efficiency [9, 10]. Having a tertiary amine in the equatorial position thereby significantly enhances the cytotoxicity of these compounds. To further investigate the molecular mode of action of these drugs, we decided to synthesize an extended set of doxorubicin analogs and study their biological activity and function. These analogs can be divided into three subsets: *1.* doxorubicin and its dimethylated analogs; *2.* non-basic analogs to study the presence of the amine on the 3' position; and *3.* cyclic-doxorubicin analogs to extent the variation of the tertiary amine features.

In line with previous data [9, 10], all four cyclic-doxorubicin analogs are very effective histone evictors abstained from the DNA damage capacity, with IC_{50} values in the

nanomolar range in multiple tumor cell lines. The opposite observation was made for the non-basic analogs, being effective DNA damage inducers without the ability to induce chromatin damage. These compounds are also less effective anticancer drugs *in vitro*. Nevertheless, all doxorubicin variants in this set are capably of re-localizing Topo IIα.

An unconsidered feature of anthracycline drugs is the genomic location where they are active. Earlier studies showed that daunorubicin induced histone eviction at distinct genomic areas from those targeted by aclarubicin [5, 7]. Therefore, here we evaluated the genomic selectivity of both the Topo IIα targeting and the site of histone eviction of the new set of analogs and identify doxorubicin variants with distinct genome specificity.

In summary, the modification of the sugar moiety at the 3' position is important for the biological activity of the anthracycline drugs. In addition, the different doxorubicin analogs show distinct genomic selectivity for their Topo IIα targeting and chromatin damage activity. Exploring the chemical space around doxorubicin leads to novel insights allowing further improvement of this old anticancer drug.

RESULTS
Evaluating the biological activity of the doxorubicin analogs

To further understand the molecular mode of action of anthracycline drugs, we synthesized and tested a new set of 3' analogs of doxorubicin (Figure 1). Based on the previous data [8-10], we included three non-basic doxorubicin variants to study the function of the 3' amine, and four cyclic-doxorubicin analogs to determine the role of other tertiary amine variants. To investigate the capacity of these doxorubicin analogs to induce DNA damage, we treated K562 cells for 2 hour with the indicated drugs and visualized DNA double-strand break formation indirectly by detecting γH2AX by Western Blot (Figure 2A and B), and directly using constant-field gel electrophoresis (Figure 2C and D). Besides dimethylation of the amino sugar, other
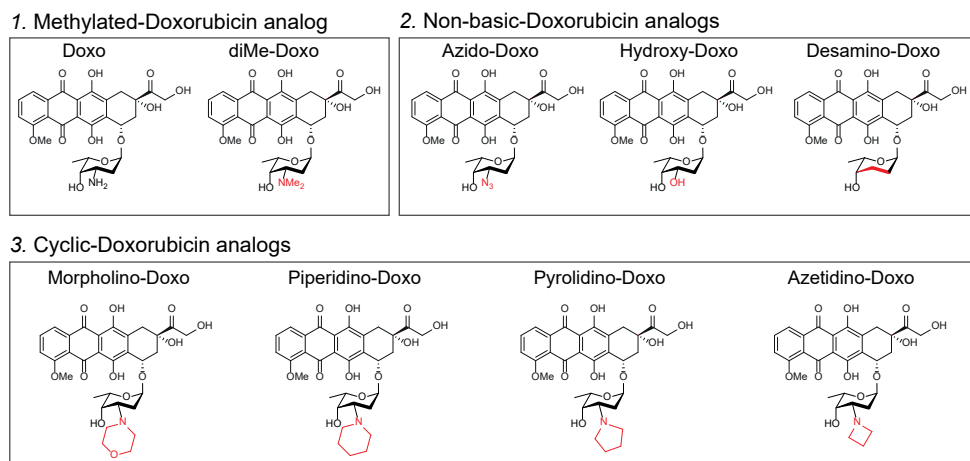
6

Figure 1. Structure of doxorubicin analogs. *The different doxorubicin analogs can be subdivided into three groups: 1. Doxorubicin and N,N-dimethyl-doxorubicin (diMe-Doxo), 2. The non-basic doxorubicin analogs and 3. The cyclic-doxorubicin analogs. In red structural differences compared to doxorubicin are indicated.*
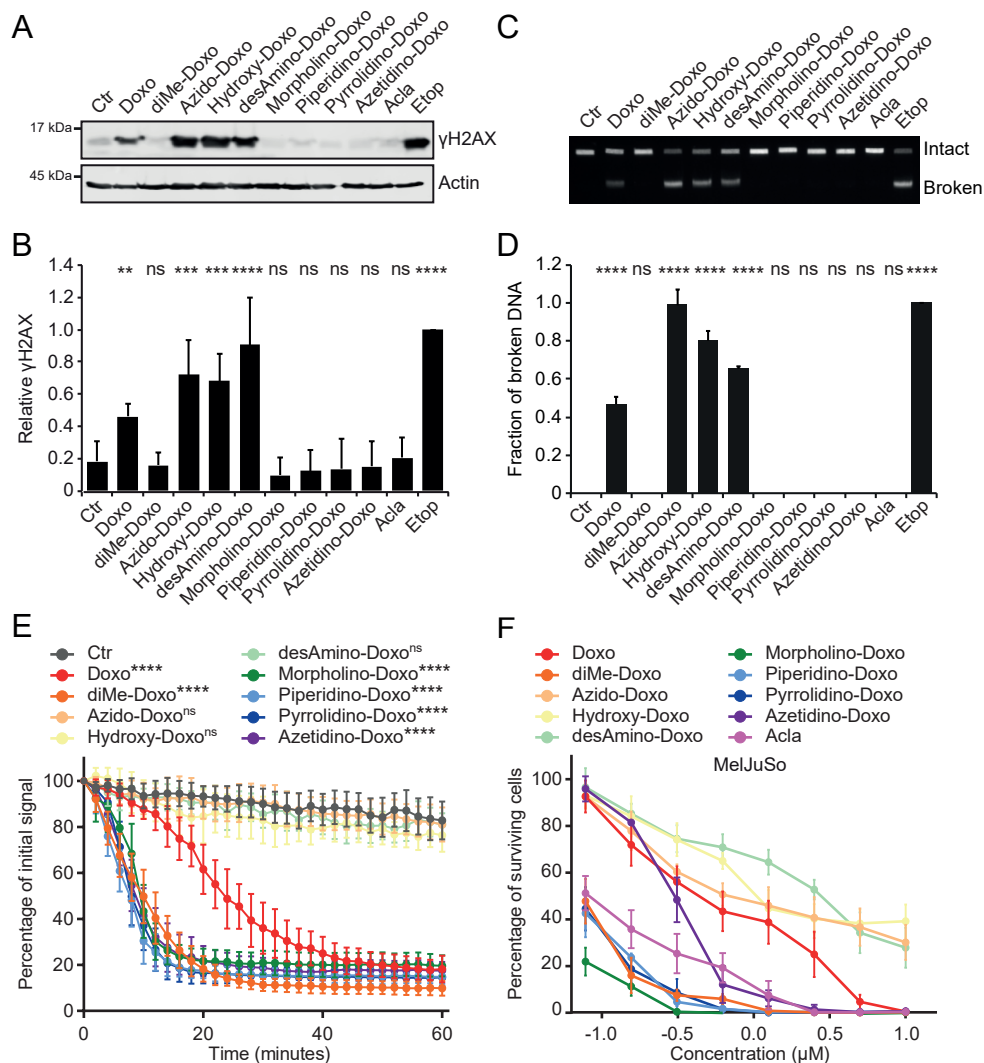
Figure 2. Biological evaluation of the doxorubicin analogs. *(A) K562 cells are treated for 2 hours with 10μM of the indicated drugs. DNA double strand breaks are visualized by γH2AX levels by Western Blot. Etoposide (Etop) and aclarubicin (Acla) were used as positive and negative control, respectively. Actin was used as a loading control. (B) Quantification of A. Results are presented as mean ± SD of three independent experiments. Ordinary one-way ANOVA with Dunnett's multiple comparison test; ns, not significant, **P < 0.01, ***P < 0.001, ****P < 0.0001. (C) K562 cells are treated for 2 hours with 10μM of the indicated drugs. DNA break formation by the various analogs was directly analyzed by CFGE. The position of intact and broken DNA is indicated. (D) Quantification of the fraction of broken DNA relative to Etop. Results are presented as mean ± SD of three independent experiments. Ordinary one-way ANOVA with Dunnett's multiple comparison test; ns, not significant, ****P < 0.0001. (E) Quantification of histone eviction measured as PAGFP-H2A release from photo-activated nuclear regions after administration of 10μM of the indicated doxorubicin analogs. Ordinary one-way ANOVA with Dunnett's multiple comparison test; ns, not significant, ****P < 0.0001.*

Figure 2. Continued. *(F) Cytotoxicity of the different doxorubicin analogs in MelJuSo cells. Cells were treated for 2 hours with the indicated concentrations followed by drug removal. Cell survival was determined 72 hours post drug removal using CellTiter-Blue assay. Data is shown as mean ± SD of three independent experiments.*

tertiary amine substitutions, as presented in the cyclic-doxorubicin analogs, are also abolished from their DNA damage activity. The three non-basic variants lacking the 3' amine are effective DNA damaging compounds. We then continued to investigate the histone eviction capacity of the doxorubicin variants. To do so, we followed the fluorescence intensity of photo-activated GFP-H2A histones (PAGFP-H2A) in MelJuSo cells upon treatment with the different drugs (Figure 2E and Figure S1). All analogs containing a tertiary amine at the 3' position were effective histone evicting compounds compared to their parental drug, while the non-basic compounds were unable to evict histones. We have thus generated doxorubicin analogs that either effectively induce DNA damage without evicting histones (Azido-Doxo, Hydroxy-Doxo and Desamino-Doxo), or variants that are unable to induce DNA double-strand breaks while being effective histone evictors (diMe-Doxo, Morpholino-Doxo, Piperidino-Doxo, Pyrolydino-Doxo and Azetidino-Doxo). This indicates that the absence/presence of a tertiary amine at the 3' position determines the DNA- and chromatin damage activities of the doxorubicin analogs.

Cytotoxicity of the doxorubicin analogs

Earlier, we showed that the effectivity of histone eviction correlated with the cytotoxicity of the compounds *in vitro* [9, 10]. Therefore, we continued to test the anticancer potential of the newly synthesized doxorubicin analogs. MelJuSo cells were treated for 2 hours with different concentrations of the various drugs, and cell viability was determined 72 hours post treatment using CellTiter-Blue. Again, the compounds with chromatin damage activity are more cytotoxic, while the non-basic doxorubicin variants (with DNA damage activity only) are the least effective anticancer drugs (Figure 2F). The cyclic-doxorubicin analogs Morpholino-Doxo, Piperidono-Doxo and Pyrolydino-Doxo were even more cytotoxic than their parental drug doxorubicin or aclarubicin, tested in 14 tumor cell lines (Table 1 and Figure S2A). In line with previous data, the histone eviction effectivity strongly correlates with cytotoxicity for this set of doxorubicin analogs (Figure S2B).

Genomic selectivity for the chromatin damage activity of the doxorubicin variants

Histone eviction by the anthracyclines daunorubicin and aclarubicin occurs in different epigenomic regions of the genome, effectively defining anthracycline drugs as region-specific epigenetic modifiers [7]. The released histones are degraded and replaced by new nascent histones, resulting in epigenomic and transcriptional changes [5, 7]. We hypothesize that this genomic specificity is determined by features within the anthracycline structure. Therefore, we assessed the different drugs for their genomic location of histone eviction. To address this, we performed ATAC-sequencing (ATAC-seq) on K562 cells treated with doxorubicin, the clinically used doxorubicin homologues daunorubicin and epirubicin, aclarubicin, amrubicin, the most cytotoxic doxorubicin isomeric analog diMe-Epi [10], and the newly synthesized doxorubicin analogs that showed chromatin damage activity (Figure 3A). ATAC-seq identifies open chromatin segments, which include histone-evicted regions [11, 12]. Overall genomic regions showing drug-specific ATAC-seq signals for the different

IC$_{50}$ (µM) / Cells	Doxo	diMe-Doxo	Azido-Doxo	Hydroxy-Doxo	desAmino-Doxo	Morpholino-Doxo	Piperidino-Doxo	Pyrolydino-Doxo	Azetidino-Doxo	Acla
A549	0.408	< 0.078	0.902	2.927	7.723	0.098	0.070	0.042	0.191	0.048
BT474	5.765	0.516	> 10.0	> 10.0	> 10.0	0.194	0.197	0.221	0.741	0.375
BXPC3	3.818	0.193	7.998	> 10.0	> 10.0	0.099	0.118	0.211	0.591	0.289
DU145	0.566	0.282	0.346	1.295	3.106	0.079	0.187	0.291	0.832	0.350
FM3	0.601	< 0.078	3.022	6.094	9.742	0.119	0.107	0.093	0.136	0.083
HCT116	0.666	0.103	0.872	1.746	5.210	0.079	0.136	0.099	0.300	0.110
Hela	0.149	0.075	0.405	1.054	3.770	0.065	0.128	0.094	0.239	0.179
K562	0.346	0.122	0.636	0.849	1.049	0.064	0.150	0.100	0.302	0.532
MelJuSo	0.523	0.073	1.224	1.904	2.430	0.051	0.078	0.073	0.297	0.099
PC3	0.829	0.166	0.888	2.786	8.294	0.033	0.120	0.189	0.532	0.225
SKBR3	1.449	0.251	> 10.0	8.892	> 10.0	0.069	0.164	0.215	0.733	0.418
U2Os	0.339	0.056	> 10.0	6.793	> 10.0	0.077	0.105	0.122	0.159	0.209
U87	0.455	< 0.078	2.032	> 10.0	9.468	0.058	0.048	0.041	0.103	0.112
U118	1.152	0.080	1.758	5.217	8.708	0.067	0.080	0.126	0.091	0.188

Table 1. Cytotoxicity of the different doxorubicin analogs *in vitro*. *Color code table of IC$_{50}$ values of the different doxorubicin analogs in various tumor cell lines in vitro. Cells were treated for 2 hours with the indicated concentrations followed by drug removal. Cell survival was determined 72 hours post drug removal using CellTiter-Blue assay. Grey bars indicate that IC$_{50}$ values are either higher or lower than the concentration tested.*

compounds nicely separates the histone evicting drugs from amrubicin (only DNA damage activity) and the untreated sample, which is illustrated by a principle component analysis (PCA; Figure 3B). When we further filter the called peaks for the control peaks (Figure S3A) and plotted the fold change of upregulated peaks compared to untreated samples (Figure 3C) the drugs were separated in three groups; i. no histone eviction (ctr and amrubicin), ii. the analogs capable of both eviction of histones and DNA damage activity (doxorubicin, daunorubicin and epirubicin), and iii. the analogs with effective histone eviction activity only (aclarubicin, diMe-Epi, diMe-Doxo, Morpho-doxo, Piperidino-doxo, Pyrolidino-doxo, Azetidino-doxo). All analogs featuring a tertiary amine at the 3' position of the sugar moiety are clustered by principle component 1, where aclarubicin (which has a different aglycon, and two additional sugar moieties) is most separated from the other doxorubicin analogs by principle component 2 (Figure 3C and S3B). However, the other doxorubicin variants also show some dispersion for principle component 2. A more detailed analyses is required to define the exact regions targeted by the various drugs, but, redirecting the various anthracycline analogs to different genomic regions is possible by modifying the 3' amino sugar.

Genomic selectivity of topoisomerase IIα targeting

The classical mechanism of action of the anthracycline drugs, is poisoning the catalytic cycle of Topo IIα, and thereby inducing DNA damage. Therefore we wondered whether the new doxorubicin analogs also target Topo IIα in specific regions in the genome; and if so, can we determine the structural features that might be responsible for this function? To test this, the nuclear localization of GFP-tagged Topo IIα was followed using time-laps confocal microscopy upon treatment with the different drugs. At steady state, Topo IIα is localized in the nucleus where it accumulates in nucleoli, but upon treatment the protein rapidly re-localized (Figure 4A and B, and Figure S4). While re-localization was observed for doxorubicin as well as all the other analogs, localizations of Topo IIα was different upon treatment with the doxorubicin variants.
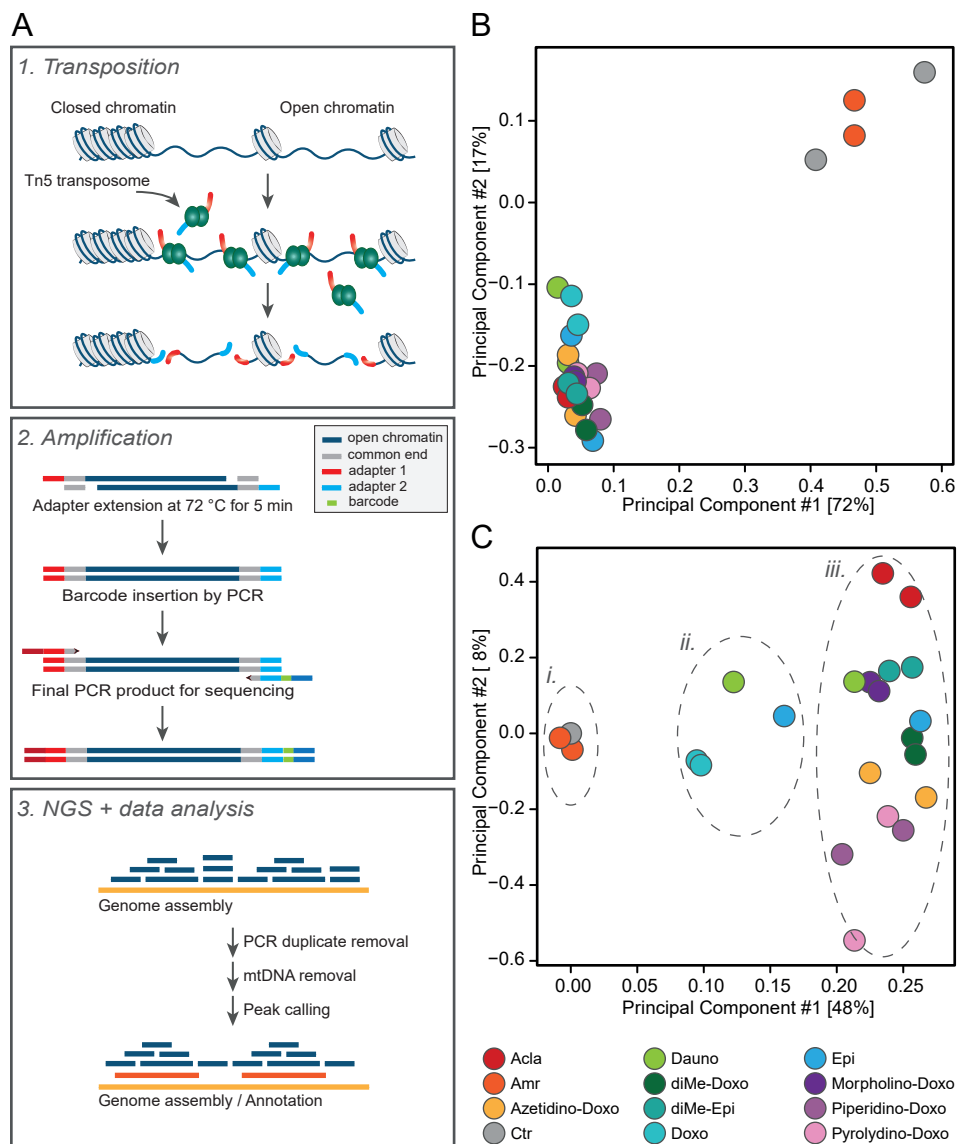
Figure 3. Doxorubicin analogs evict histones in unique genomic regions. *(A) Schematic representation of the ATAC-seq workflow: 1. The Tn5 transposome is able to access open chromatin regions and introduce its preloaded NGS adapters, thereby generating the ATAC-seq library. 2. After DNA purification, the adapters are extended and barcodes are inserted using PCR to prepare the library for sequencing. 3. The resulting DNA can be analyzed by qPCR and/or next generation sequencing (NGS). PCR duplicates and mitochondrial DNA (mtDNA) were removed using different bioinformatic packages after which the genomic locations of the open chromatin can be identified. (B) Principle Component Analysis (PCA) of total ATAC-seq peak calls, overall signal (RPKM counts) no filters were applied. (C) PCA of the fold change of upregulated peaks compared to ctr. Separation of the drugs in three groups; i. no histone eviction (ctr and amrubicin), ii. the analogs capable of both histone eviction and DNA damage*

Figure 3. Continued (C). *activity (doxorubicin, daunorubicin and epirubicin), iii. the analogs with effective histone evicting activity only (Acla, diMe-Epi, diMe-Doxo, morpho-doxo, piperidino-doxo, pyrolidino-doxo, azetidino-doxo). ATAC-seq peak calls were extracted with the EN-CODE ATAC-seq analysis pipeline.*
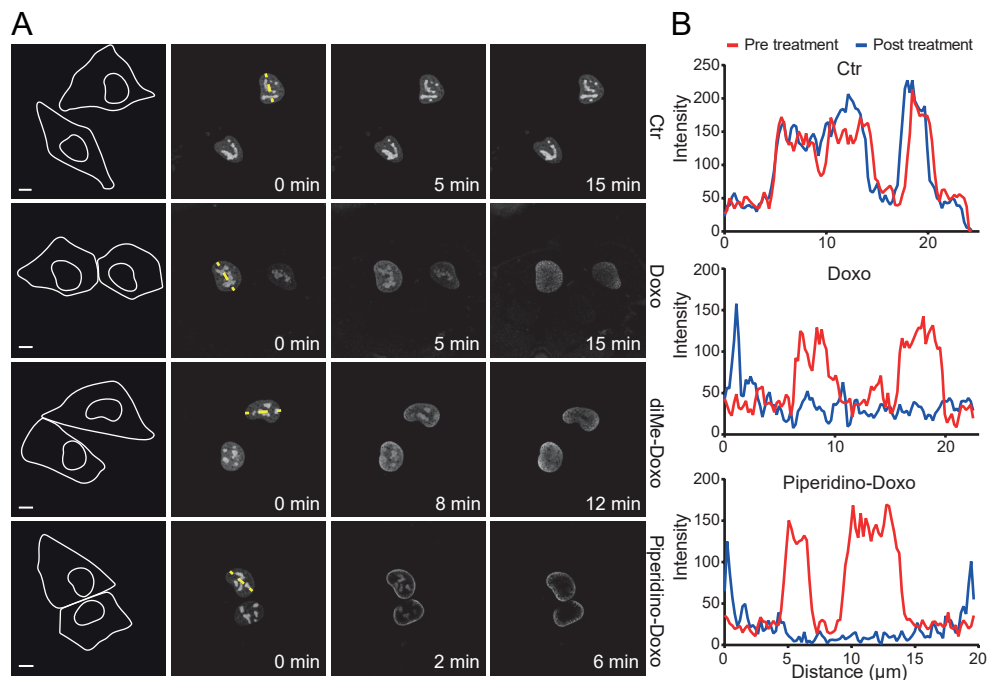

Figure 4. Topoisomerase IIα relocalization. *Relocalization of GFP-Topo IIα transiently expressed in MelJuSo cells. (A) Cells are treated with 10μM of the indicated doxorubicin analogs and followed over time. Lines in the left panel define the cytoplasm and nucleus. Stills at indicated time points from time-laps experiment are shown. Scale bar, 10μm. (B) Pixel plot of the GFP signal pre- and post treatment with the drugs. Plotted as fluorescence over distance of dotted yellow line as marked in (A).*

Especially the cyclic-doxorubicin analogs targeted the protein to the outer side of the nucleus, compared to the other analogs, which re-mobilized Topo IIα more equal over the whole nucleus. To determine, at a higher resolution, the genomic location of Topo IIα trapped by the various analogs, we generated an endogenous 3xFLAG-tagged Topo IIα K562 cell line (Figure S5). Subsequently, these cells were treated with the different drugs and analyzed by ChIP-sequencing (ChIP-seq; Figure 5A). The overall ChIP-seq signal revealed three main drug clusters, which is illustrated by PCA of the total ChIP-seq peaks called (Figure 5B). The first cluster *(i.)* constitutes mainly of analogs able to induce both DNA- and chromatin damage, and the non-basic doxorubicin analogs with DNA damage activity only. The second group *(ii.)* is formed by aclarubicin and most of the doxorubicin analogs that are very effective histone evictors (all featuring a tertiary amine at the 3' position), while amrubicin, the structurally unrelated Topo IIα inhibitor etoposide, and the untreated control sample form the third group *(iii.)*. When called peaks are filtered for ctr peaks, the third cluster formed by the untreated cells, etoposide and amrubicin disappeared, indicating that both etoposide and amrubicin target Topo IIα at the location where the enzyme
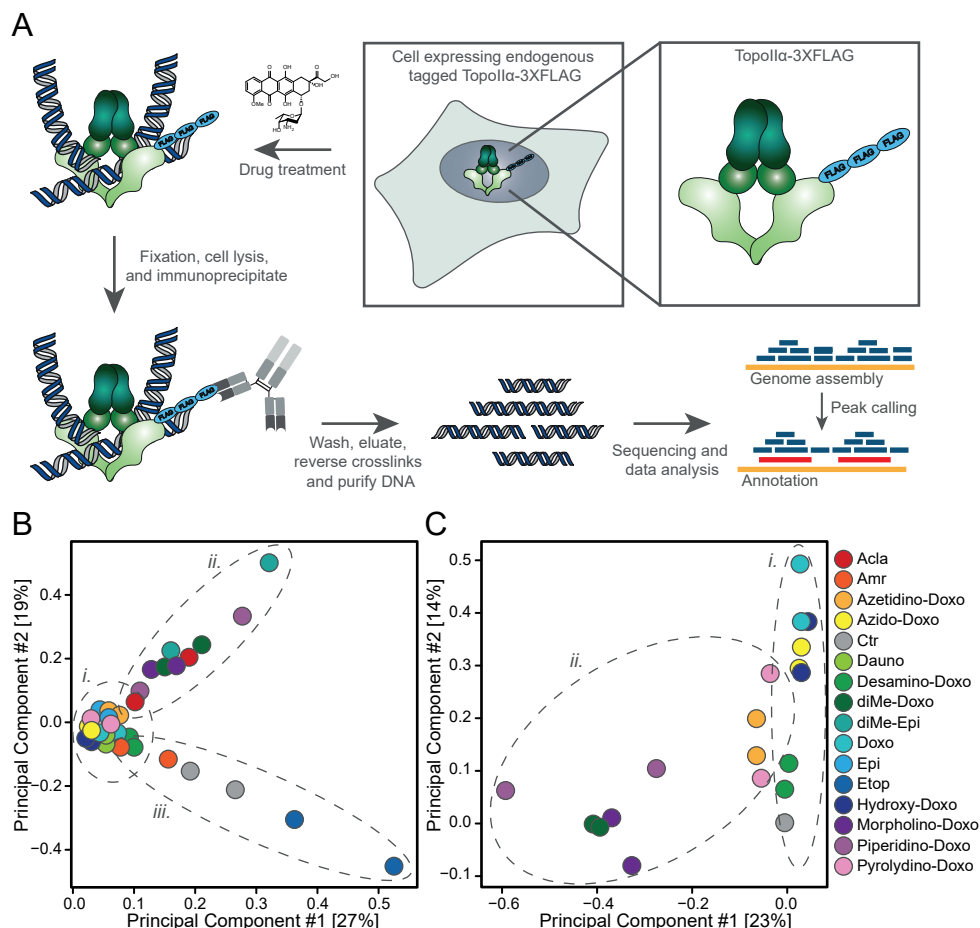
Figure 5. Doxorubicin analogs alter genomic location of topoisomerase IIα. *(A) Schematic representation of Topo IIα ChIP-seq experiment. K562 cells endogenously expressing 3xFLAG-tagged Topo IIα were treated with the indicated drugs followed by fixation, cell lysis and immunoprecipitation using FLAG antibody. Subsequently, Topo IIα bound DNA was isolated, sequenced and analyzed. (B) Principle Component Analysis (PCA) of total ChIP-seq peak calls, overall signal (RPKM counts) no filters were applied. (i.) main cluster of analogs able to both induce DNA- and chromatin damage, the non-basic doxorubicin analogs with DNA damage activity only and pyrolidino-doxorubicin. (ii.) aclarubicin and most of the doxorubicin analogs featuring a tertiary amine at the 3' position. (iii.) ctr, etoposide and amrubicin. (C) PCA of the fold change of upregulated peaks compared to ctr of a selection of the samples (doxorubicin analogs). ChIP-seq peak calls were extracted with the ENCODE ChIP-seq analysis pipeline. (i.) the DNA damaging doxorubicin analogs, featuring a primary amine or non-basic side group (ii.) the histone eviction only doxorubicin analogs with tertiary amine.*

performs its biological function (Figure S6A). Further analysis by plotting the normalized data (fold change compared to ctr) separates the DNA damaging compounds *(i.)* from the histone evicting drugs *(ii.)* (Figure 5C and S6B). This suggest that the different analogs trap Topo IIα at different genomic regions, and that these regions may be determined by their structure and ability to induce DNA- or chromatin damage.

CONCLUSION AND FUTURE DIRECTIONS

Although the anthracycline drugs are used in the clinic for over five decades to treat various types of cancer, detailed understanding of their structure – function relationship is limited. Therefore, studying the biological consequence of novel analogs can be valuable in understanding their exact molecular mechanism. Based on previous data, the methylation status and orientation of the 3' amine of the compound appeared to be important for the biological function. Therefore, we aimed to further decipher the effects of modifications on this chemical group. To do so, we synthesized various doxorubicin analogs featuring novel side groups at this amino sugar 3' position, resulting in three non-basic and four cyclin-doxorubicin analogs. Biological evaluation of this set of compounds suggests that the tertiary amine on this 3' position is responsible for the chromatin damage capacity of these structures. All four cyclic-doxorubicin analogs were, like diMe-Doxo, equally effective histone evicting compounds and show overall similar cytotoxicity, without inducing DNA double-strand breaks. While the non-basic doxorubicin analogs were unable to evict histones, they still were, similar to their parental drug, effective DNA damaging compounds. Although the compounds differed in their biological activity, all doxorubicin variants remained capable to re-locate Topo IIα in the nucleus of living cells. Identification of the genomic regions where Topo IIα was trapped by the different compounds, as detected by ChIP-seq, indicate that these drugs can be clustered in two main groups. The anthracycline analogs that poison Topo IIα and thereby produce DNA damage likely target Topo IIα at the genomic locations where the enzyme performs it's biological function, while the other analogs, more specialized in histone eviction, seem to redirect Topo IIα to other genomic regions. The microscopy data indicate that the doxorubicin variants containing a tertiary amine relocated Topo IIα more to the genomic regions close to the nuclear envelop. However, further detailed evaluation of these genomic regions is necessary to define their genomic selectivity and understand the biological consequence of this difference. Comparable results were obtained for the chromatin damage activity for the doxorubicin analogs by ATAC-seq analysis. Histone eviction is induced at different genomic locations, which can be linked to their chemical structure. The analogs featuring a tertiary amine (aclarubicin, Azetidino-doxo, diMe-Doxo, diMe-Epi, Morpholino-doxo, Pyrolidino-doxo and Piperidino-doxo) are all very effective histone evicting drugs, and seem to induce chromatin damage at a distinct genomic regions from the analogs with a primary amine at the 3'position, which have both DNA damage and chromatin damage activity (doxorubicin, epirubicin and daunorubicin) and from amrubicin, which is unable to evict histones.

A more detailed analysis of the genomic selectivity of these analogs could help to better understand the structure-function relationship of anthracycline drugs, which could help with predicting the effectivity of particular tumors types (with e.g. epigenetic alterations) for specific anthracycline analogs. Exploring the chemical space around doxorubicin resulted in potential novel drug variants with distinct structure-function relationship and genomic selectivity, which can help in the development of improved anthracycline-based cancer therapies.

MATERIALS AND METHODS
Reagents and antibodies
Doxorubicin was obtained from Accord Healthcare Limited, UK, etoposide was obtained from Pharmachemie (the Netherlands), aclarubicin (sc-200160) was pur-

chased from Santa Cruz Biotechnology (USA), diMe-doxo was obtained via synthesis as described before [8]. The doxorubicin analogs were synthesized as described [13]. Primary antibodies used for Western blotting: γH2AX (1:1000, 05-036, Millipore), β-actin (1:10000, A5441, Sigma). Secondary antibody used for blotting: IRDye 800CW goat anti-mouse IgG (H+L) (926-32210, Li-COR, 1:10000).

Cell culture and constructs

K562 cells (B. Pang, Stanford University, USA), HCT116 cells (T. van Hall, LUMC, The Netherlands), BXPC-3 cells (ATCC® CRL-1687), PC3 and DU145 cells (C. Robson, Newcastle University, UK), were maintained in RPMI-1640 medium supplemented with 8% FCS. A549 cells (R. Bernards, NKI, The Netherlands), FM3 cells (D. Peeper, NKI, The Netherlands), U87 MG (ATCC® HTB-14), U118 MG (ATCC® HTB-15), U2Os cells (ATCC® HTB-96), Hela cells (ATCC® CCL-2) and SKBR3 (R. Beijersbergen, NKI, The Netherlands), were maintained in DMEM medium supplemented with 8% FCS. BT474 cells (R. Beijersbergen, NKI, The Netherlands) were maintained in DMEM/F12 medium supplemented with 8% FCS. MelJuSo cells were maintained in IMDM medium supplemented with 8% FCS. MelJuSo cells stably expressing PAGFP-H2A were maintained in IMDM supplemented with 8% FCS and G-418, as described [5]. Endogenous tagged 3xFLAG-Topo IIα K562 cell lines were generated using homology repair 3xFLAG constructs designed at least 40 base pairs up and downstream of the genomic topoisomerase IIα stop codon. The gRNA target sequence was designed using the ZANG Lab CRISPR tool (http://crispr.mit.edu/) and cloned into the pX330 vector. Primers used for the HR construct: 5' CACCGAT-GATCTGTTTTAAAATGTG 3' and 5' AAACCACATTTTAAAACAGATCATC 3'. Co-transfection of ssDNA oligo and CRISPR plasmid (CRISPR sequence into pX459) into K562 cells by electroporation using Lonza SF cell line kit. Primers used for genotyping: Topo IIα fwd: TAAGCAGAATTCATGCCACTTATTGGGCAAT and Topo IIα rev: TGCTTAAAGCTTTGCCCATGAGATGGTCACTA. Cell lines were maintained in a humidified atmosphere of 5% CO_2 at 37°C and regularly tested for the absence of mycoplasma. Topo IIα-GFP construct was described before [5].

Confocal microscopy

For PAGFP-H2A photoactivation and time-lapse confocal imaging cells were seeded in a 35mm glass bottom petri dish (Poly-dlysine-Coated, MatTek Corporation), and imaged 16 hours later as described [5]. For live cell imaging of GFP-Topo IIα, MelJuSo cells were seeded in a 35mm glass bottom petri dish (Poly-dlysine-Coated, MatTek Corporation), transfected (effectene, Qiagen) 16 hours later and treated as indicated. Time-lapse confocal imaging was performed on a Leica SP8 confocal microscope system, 63x lens, equipped with a climate chamber. Images were quantified using Image J software.

Western blot and constant-field gel electrophoresis (CFGE)

Cells were treated with drugs at indicated dose for 2 hours. Subsequently, drugs were removed by extensive washing and cells were collected and processed immediately for the assays. For Western blot cells were lysed directly in SDS-sample buffer (2% SDS, 10% glycerol, 5% β-mercaptoethanol, 60mM Tris-HCl pH 6.8 and 0.01% bromophenol blue). Lysates were resolved by SDS/polyacrylamide gel electrophoresis followed by western blotting. Primary antibodies used for blotting: γH2AX (1:1000, 05-036, Millipore) and β-actin (1:10000, A5441, Sigma). For CFGE: DNA double strand breaks were quantified by constant-field gel electrophoresis as

6

described [14]. Images were quantified using ImageJ software.

In vitro cell viability assay

Cells were seeded into 96-well format. Twenty-four hours after seeding, cells were treated with indicated drugs for 2 hours at various concentrations. Subsequently, drugs were removed and cells were left to grow for an additional 72 hours. Cell viability was measured using the CellTiter-Blue viability assay (Promega). Relative survival was normalized to the untreated control and corrected for background signal.

Topo IIα ChIP sequencing

A total of 5×10^7 endogenous tagged 3xFLAG-Topo IIα K562 cells per sample were treated with 10μM of the indicated drugs for 4 hours. The experiments were performed with biological replicates. Cells were fixed and processed as described [15, 16]. For ChIP-seq, the mouse anti-FLAG M2 (F3165, Sigma) was used. Sequencing was done on a Illumina Hiseq2000 platform (Genome Sequencing Service Center of Stanford Center for Genomics and Personalized Medicine Sequencing Center). All samples were quality controlled and processed identically using the available ChIP-seq peak calling pipeline published by ENCODE, version 0.2.0 (https://github.com/ENCODE-DCC/chip-seq-pipeline2). Peak normalization and contrasts to control samples was performed using the package DiffBind for R statistical computing software [17].

Epigenomic profiling of histone eviction regions by ATAC-sequencing

A total of 5×10^4 K562 cells per sample were treated with 10 μM of the indicated drugs for 4 hours. The experiments were performed with biological replicates. For ATAC-seq, after treatment cells were fixed and processed as described [11, 18]. DNA was processed using a customized library preparation method for ATAC-seq as described and was sequenced using an Illumina HiSeq4000 platform. All samples were quality controlled and processed identically using the available ATAC-seq peak calling pipeline published by ENCODE, version 0.3.0 (DOI: 10.5281/zenodo.156534). Peaks were annotated with epigenomic signatures of K562, downloaded from ENCODE Project [19]. Peak normalization and contrasts to control samples was performed using the package DiffBind for R statistical computing software [17].

Quantification and statistical analysis

Each experiment was assayed in triplicate, unless stated otherwise. All error bars denote ±SD. Statistical analyses was performed using Prism 8 software (GraphPad Inc.). ns, not significant, *$p < 0.05$, **$p < 0.01$, ***$p < 0.001$, ****$p < 0.0001$.

REFERENCES

1. Lotrionte, M., Biondi-Zoccai, G., Abbate, A., Lanzetta, G., D'Ascenzo, F., Malavasi, V., Peruzzi, M., Frati, G. & Palazzoni, G. (2013) Review and meta-analysis of incidence and clinical predictors of anthracycline cardiotoxicity, Am J Cardiol. 112, 1980-4.
2. Mistry, A. R., Felix, C. A., Whitmarsh, R. J., Mason, A., Reiter, A., Cassinat, B., Parry, A., Walz, C., Wiemels, J. L., Segal, M. R., Ades, L., Blair, I. A., Osheroff, N., Peniket, A. J., Lafage-Pochitaloff, M., Cross, N. C., Chomienne, C., Solomon, E., Fenaux, P. & Grimwade, D. (2005) DNA topoisomerase II in therapy-related acute promyelocytic leukemia, N Engl J Med. 352, 1529-38.

3. Weiss, R. B. (1992) The Anthracyclines - Will We Ever Find a Better Doxorubicin, Semin Oncol. 19, 670-686.

4. Nitiss, J. L. (2009) Targeting DNA topoisomerase II in cancer chemotherapy, Nat Rev Cancer. 9, 338-350.

5. Pang, B., Qiao, X., Janssen, L., Velds, A., Groothuis, T., Kerkhoven, R., Nieuwland, M., Ovaa, H., Rottenberg, S., van Tellingen, O., Janssen, J., Huijgens, P., Zwart, W. & Neefjes, J. (2013) Drug-induced histone eviction from open chromatin contributes to the chemotherapeutic effects of doxorubicin, Nature communications. 4, 1908.

6. Yang, F., Kemp, C. J. & Henikoff, S. (2013) Doxorubicin enhances nucleosome turnover around promoters, Curr Biol. 23, 782-7.

7. Pang, B., de Jong, J., Qiao, X., Wessels, L. F. & Neefjes, J. (2015) Chemical profiling of the genome with anti-cancer drugs defines target specificities, Nat Chem Biol. 11, 472-80.

8. Qiao, X., van der Zanden, S. Y., Wander, D. P. A., Borras, D. M., Song, J. Y., Li, X., van Duikeren, S., van Gils, N., Rutten, A., van Herwaarden, T., van Tellingen, O., Giacomelli, E., Bellin, M., Orlova, V., Tertoolen, L. G. J., Gerhardt, S., Akkermans, J. J., Bakker, J. M., Zuur, C. L., Pang, B., Smits, A. M., Mummery, C. L., Smit, L., Arens, R., Li, J., Overkleeft, H. S. & Neefjes, J. (2020) Uncoupling DNA damage from chromatin damage to detoxify doxorubicin, Proc Natl Acad Sci U S A.

9. Dennis P. A. Wander , S. Y. v. d. Z., Gijsbert A. van der Marel, Herman S. Overkleeft, Jeroen D. C. Codée, Jacques Neefjes (2020) Doxorubicin and Aclarubicin: Shuffling Anthracycline Glycans for Improved Anti-Cancer Agents, Chapter 4.

10. Dennis P. A. Wander, S. Y. v. d. Z., Merijn B. L. Vriends, Branca C. van Veen, Joey G. C. Vlaming, Thomas Bruyning, Gijsbert A. van der Marel, Herman S. Overkleeft, Jacques Neefjes, Jeroen D. C. Codée (2020) Synthetic (N,N-dimethyl)doxorubicin Glycosyl Diastereomers to Dissect Modes of Action of Anthracycline Anticancer Drugs, Chapter 5.

11. Buenrostro, J. D., Giresi, P. G., Zaba, L. C., Chang, H. Y. & Greenleaf, W. J. (2013) Transposition of native chromatin for fast and sensitive epigenomic profiling of open chromatin, DNA-binding proteins and nucleosome position, Nat Methods. 10, 1213-+.

12. Giresi, P. G., Kim, J., McDaniell, R. M., Iyer, V. R. & Lieb, J. D. (2007) FAIRE (Formaldehyde-Assisted Isolation of Regulatory Elements) isolates active regulatory elements from human chromatin, Genome Res. 17, 877-85.

13. Wander, D. P. A. (2019) Synthesis of a Focused Library of Doxorubicin/Aclarubicin - Inspired Structures.

14. Wlodek, D., Banath, J. & Olive, P. L. (1991) Comparison between Pulsed-Field and Constant-Field Gel-Electrophoresis for Measurement of DNA Double-Strand Breaks in Irradiated Chinese-Hamster Ovary Cells, Int J Radiat Biol. 60, 779-790.

15. Schmidt, D., Wilson, M. D., Spyrou, C., Brown, G. D., Hadfield, J. & Odom, D. T. (2009) ChIP-seq: Using high-throughput sequencing to discover protein-DNA interactions, Methods. 48, 240-248.

16. Pang, B. X., de Jong, J., Qiao, X. H., Wessels, L. F. A. & Neefjes, J. (2015) Chemical profiling of the genome with anti-cancer drugs defines target specificities, Nat Chem Biol. 11, 472-+.

17. Ross-Innes, C. S., Stark, R., Teschendorff, A. E., Holmes, K. A., Ali, H. R., Dunning, M. J., Brown, G. D., Gojis, O., Ellis, I. O., Green, A. R., Ali, S., Chin, S. F., Palmieri, C., Caldas, C. & Carroll, J. S. (2012) Differential oestrogen receptor binding is associated with clinical outcome in breast cancer, Nature. 481, 389-U177.

6

18. Corces, M. R., Trevino, A. E., Hamilton, E. G., Greenside, P. G., Sinnott-Armstrong, N. A., Vesuna, S., Satpathy, A. T., Rubin, A. J., Montine, K. S., Wu, B., Kathiria, A., Cho, S. W., Mumbach, M. R., Carter, A. C., Kasowski, M., Orloff, L. A., Risca, V. I., Kundaje, A., Khavari, P. A., Montine, T. J., Greenleaf, W. J. & Chang, H. Y. (2017) An improved ATAC-seq protocol reduces background and enables interrogation of frozen tissues, Nat Methods. 14, 959-+.

19. Pazin, M. J. (2015) Using the ENCODE Resource for Functional Annotation of Genetic Variants., Cold Spring Harb Protoc. 2015, 522-536.

SUPPLEMENTAL INFORMATION

6
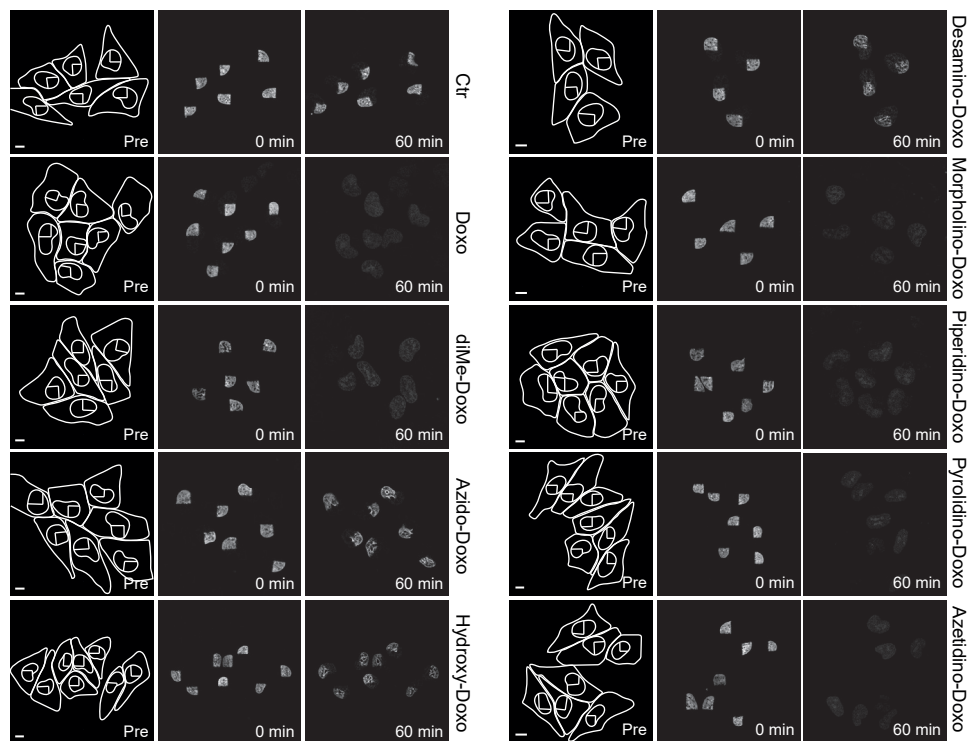
Figure S1. Chromatin damage via eviction of histone by the various doxorubicin analogs. *Part of the nucleus of MelJuSo cells stably expressing PAGFP-H2A was photo-activated and histone eviction was measured by time-lapse confocal microscopy upon administration of 10µM of the indicated compounds. Lines in the left panel define the cytoplasm, nucleus and activated region of the nucleus before treatment. Stills at indicated time points from time-lapse experiment are shown. Scale bar, 10µm.*

Figure S2. Continued (A). *Cell survival was determined 72 hours post drug removal using CellTiter-Blue assay. Data is shown as mean ± SD of three independent experiments. (B) Histone eviction speed (the time at which 25% of the initial signal is reduced) is correlated with IC_{50} of the various doxorubicin isomers. Two-tailed Pearson r correlation p = ** < 0.01.*
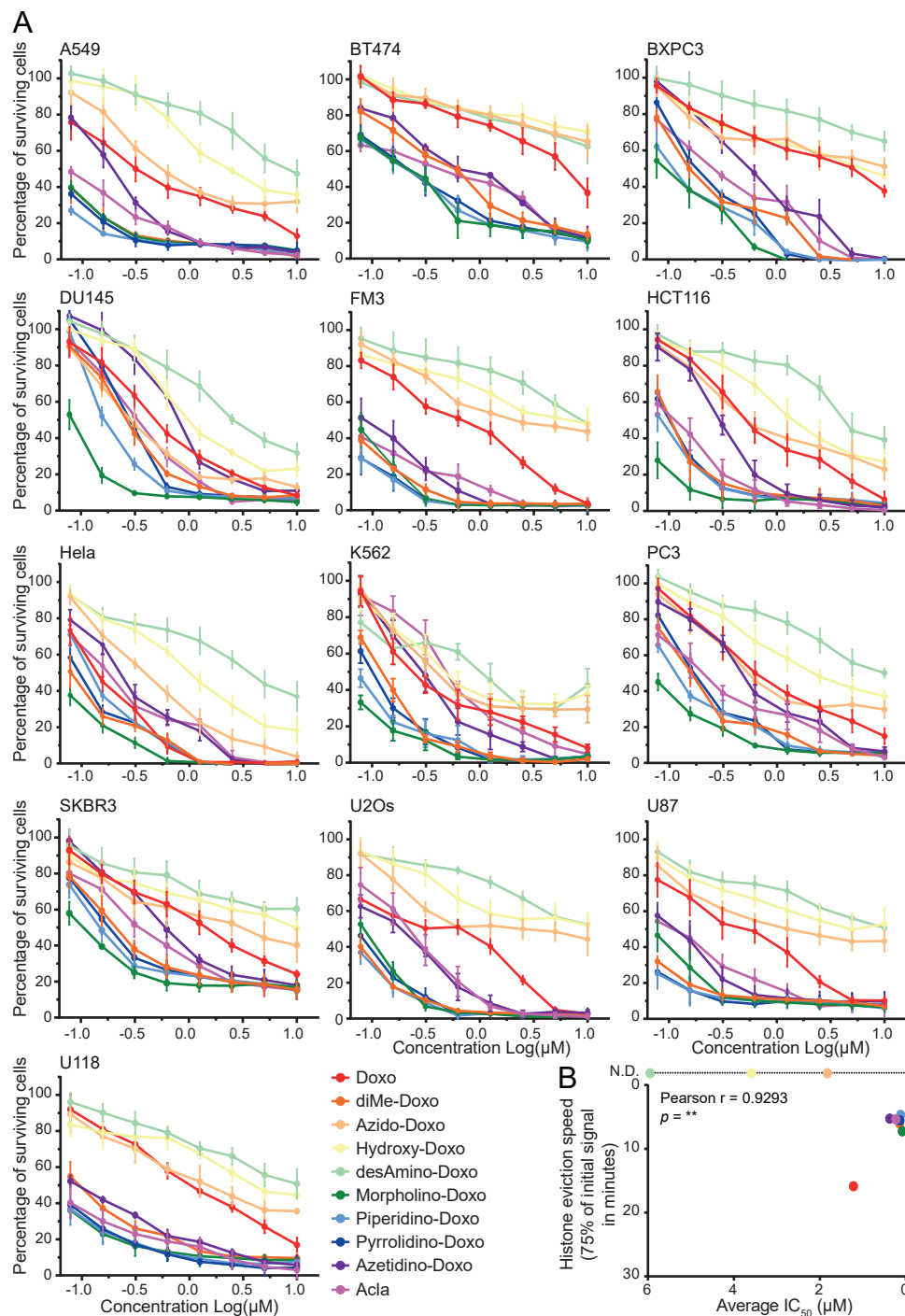
Figure S2. Cytotoxicity of the different doxorubicin analogs in various tumor cell lines.
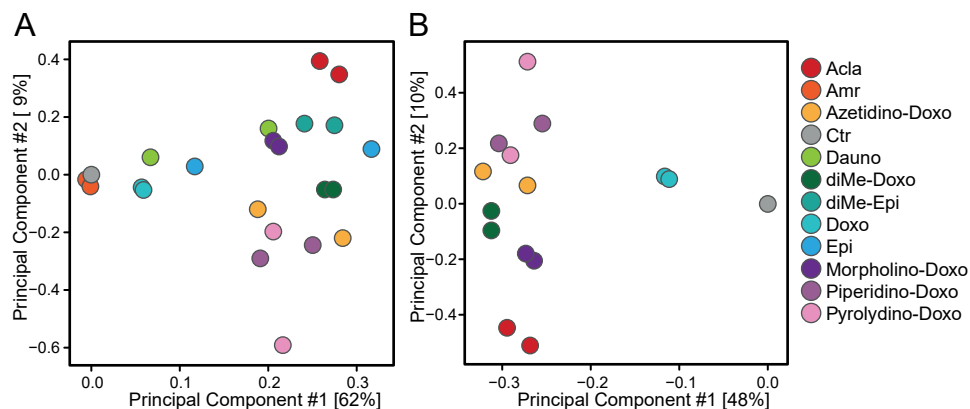*(A) Cells were treated for 2 hours with the indicated concentrations followed by drug removal.*

Figure S3. ATAC-seq analysis of chromatin damage differences. *K562 cells were treated for 4 hours with the indicated drugs and processed for ATAC-seq. (A) Principle Component Analysis (PCA) of total ATAC-seq peak calls, overall signal filtered for ctr peaks. (B) PCA of the fold change of peaks compared to ctr, a selection of the samples plotted in Figure 3C is included. ATAC-seq peak calls were extracted with the ENCODE ATAC-seq analysis pipeline.*
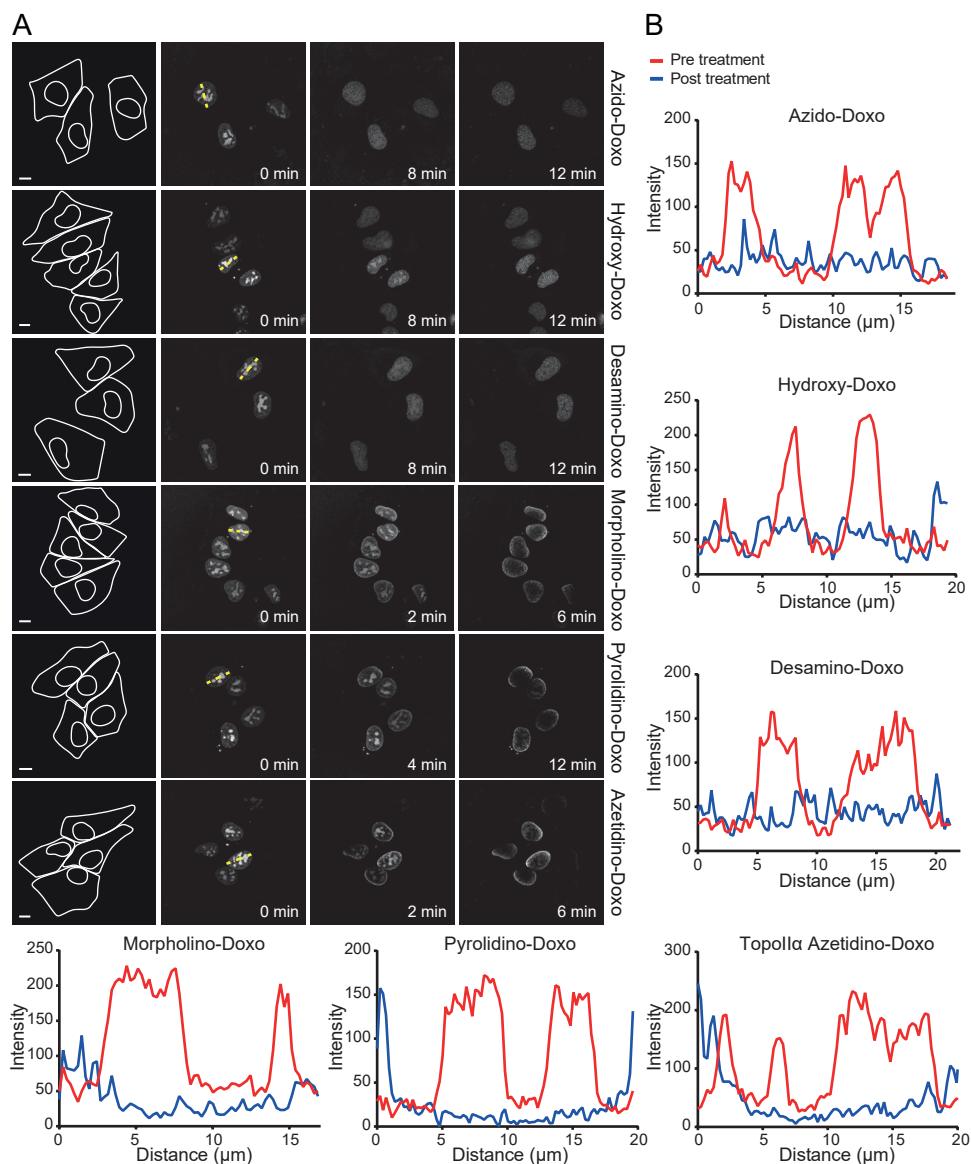
Figure S4. Topoisomerase IIα relocalization. *Relocalization of GFP-Topo IIα transiently expressed in MelJuSo cells. (A) Cells are treated with 10µM of the indicated doxorubicin ana-logs and followed over time. Lines in the left panel define the cytoplasm and nucleus. Stills at indicated time points from time-laps experiment are shown. Scale bar, 10µm. (B) Pixel plot of the GFP signal pre- and post treatment with the drugs. Plotted as fluorescence over distance of dotted yellow line as marked in (A).*
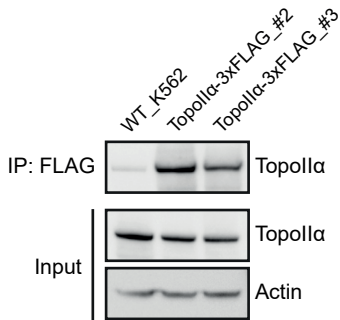
Figure S5. *Verification of endogenously tagged Topo IIα-3xFLAG K562 cell line. Wild-type and two single cell clones of Topo IIα-3xFLAG K562 cells lines were lysed and immunoprecipitated. Immunoprecipitated TopoIIα is visualized by Western blot.*
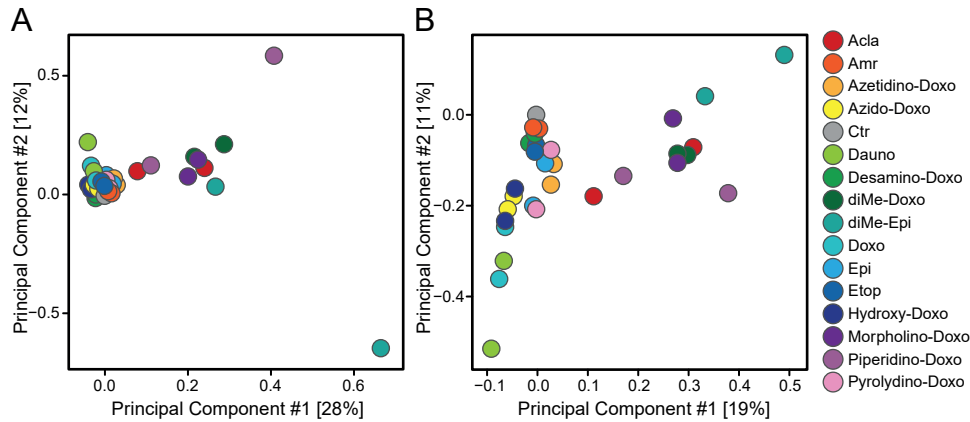

Figure S6. Differences in genomic location of TopoIIα targeting by the doxorubicin analogs. *Endogenous Topo IIα-3xFLAG K562 cells were treated for 4 hours with the indicated drugs and processes for FLAG-ChIP-seq. (A) Principle Component Analysis (PCA) of ChIP-seq peak calls, filtered for control peaks. (B) PCA of the fold change of peaks compared to ctr, all samples tested are included. ChIP-seq peak calls were extracted with the ENCODE ChIP-seq analysis pipeline.*

6